A global single-sensor analysis of 2002–2011 tropospheric nitrogen dioxide trends observed from space

P. Schneider[1] and R. J. van der A[2]

[1]   A global nine-year archive of monthly tropospheric NO_2 data acquired by the SCanning Imaging Absorption spectroMeter for Atmospheric CartograpHY (SCIAMACHY) instrument was analyzed with respect to trends between August 2002 and August 2011. In the past, similar studies relied on combining data from multiple sensors; however, the length of the SCIAMACHY data set now for the first time allows utilization of a consistent time series from just a single sensor for mapping NO_2 trends at comparatively high horizontal resolution (0.25°). This study provides an updated analysis of global patterns in NO_2 trends and finds that previously reported decreases in tropospheric NO_2 over Europe and the United States as well as strong increases over China and several megacities in Asia have continued in recent years. Positive trends of up to 4.05 ($\pm$0.41) $\times$ 10^{15} molecules cm^{-2} yr^{-1} and up to 19.7 ($\pm$1.9) % yr^{-1} were found over China, with the regional mean trend being 7.3 ($\pm$3.1) % yr^{-1}. The megacity with the most rapid relative increase was found to be Dhaka in Bangladesh. Subsequently focusing on Europe, the study further analyzes trends by country and finds significantly decreasing trends for seven countries ranging from −3.0 ($\pm$1.6) % yr^{-1} to −4.5 ($\pm$2.3) % yr^{-1}. A comparison of the satellite data with station data indicates that the trends derived from both sources show substantial differences on the station scale, i.e., when comparing a station trend directly with the equivalent satellite-derived trend at the same location, but provide quite similar large-scale spatial patterns. Finally, the SCIAMACHY-derived NO_2 trends are compared with equivalent trends in NO_2 concentration computed using the Co-operative Programme for Monitoring and Evaluation of the Long-range Transmission of Air Pollutants in Europe (EMEP) model. The results show that the spatial patterns in trends computed from both data sources mostly agree in Central and Western Europe, whereas substantial differences are found in Eastern Europe.

1. Introduction

[2]   Nitrogen dioxide (NO_2) is one of most prominent air pollutants and is emitted primarily by combustion processes resulting from transportation, industry, and power plants [*Seinfeld and Pandis*, 2006]. While NO_2 concentrations have been observed for air quality purposes at the station level for many decades, such station measurements are often limited in spatial coverage and/or density. More recently, space observations of NO_2 have become available and now allow for spatially continuous mapping of NO_2 at regional, continental, and global scales.

[3]   Operational satellite remote sensing of NO_2 has been carried out since 1995 when the Global Ozone Monitoring Experiment (GOME) [*Burrows et al.*, 1999; *Richter and Burrows*, 2002] was first launched. Beginning in 2002, the observations were continued by the SCIAMACHY (SCanning Imaging Absorption spectroMeter for Atmospheric CartograpHY) sensor onboard of Envisat [*Bovensmann et al.*, 1999; *Gottwald et al.*, 2006], and subsequently complemented in 2004 by the Ozone Monitoring Instrument (OMI) [*Levelt et al.*, 2006] as well as the Global Ozone Monitoring Experiment-2 (GOME-2) instrument in 2006 [*Munro et al.*, 2006].

[4]   The comprehensive data archive provided by these sensors allows for quantifying global and regional trends in NO_2 concentration. Several studies have investigated this, although this was always done using a combination of several sensors due to the brevity of each sensor's time series. For example, several satellite-based studies have investigated the recent increase in tropospheric NO_2 over China [*Richter et al.*, 2005; *van der A et al.*, 2006]. *Richter et al.*

[1]Norwegian Institute for Air Research, Kjeller, Norway.
[2]Royal Netherlands Meteorological Institute, De Bilt, Netherlands.

Corresponding author: P. Schneider, Norwegian Institute for Air Research, PO Box 100, NO-2027 Kjeller, Norway. (ps@nilu.no)

[2005] also found a decrease in tropospheric NO_2 emissions over parts of Europe. *van der A et al.* [2008] studied global NO_2 trends and seasonal variability from both GOME and SCIAMACHY between 1996 and 2006. Also using a combined GOME and SCIAMACHY data set in conjunction with a continental-scale air quality model, *Konovalov et al.* [2008] studied summertime trends in European NO_x emissions between 1996 and 2005. More recently, and using an updated methodology, *Konovalov et al.* [2010] also reported on summertime trends in NO_x emissions for European and Middle-Eastern megacities. Furthermore, *Kim et al.* [2006] used a combination of GOME and SCIAMACHY data to determine decreasing trends of NO_x emissions over power plants in the United States. Using a similar data set, *Ghude et al.* [2008] estimated continental-scale NO_2 trends and *Ghude et al.* [2009] provided estimates of NO_2 trends for megacities in India.

[5] Due to the, at the time, short record length of available SCIAMACHY data, all of the above mentioned studies needed to combine data from both GOME and SCIAMACHY in order to derive a time series long enough for trend analysis. At the time of this study, however, nearly a full decade of SCIAMACHY data is available and it is thus possible and worthwhile to investigate to what extent this data alone can be used to derive trends in tropospheric NO_2 concentrations. This approach avoids potential uncertainty associated with the combination of data from two different instruments, such as differences in spatial resolution, sensor calibration, local overpass time, and retrieval algorithms. More specifically, using solely SCIAMACHY data allows for the analysis of a stable and homogeneous time series generated using a consistent retrieval algorithm and in addition avoids resampling to the coarser spatial resolution of GOME data, and therefore allows for spatially more detailed trend maps.

[6] As such, the primary objective of this study is to investigate the general potential of a single-sensor 9-year SCIAMACHY data set for temporal analysis of NO_2 by mapping trends in tropospheric NO_2 column on a global scale and comparing the results with those obtained from other data sources. In this study we therefore first present an updated analysis of global tropospheric NO_2 trends between 2002 and 2011 based solely on SCIAMACHY data and subsequently focus on a Europe-wide comparison of these results with similar trends derived from station observations and from NO_2 concentrations and NO_x emissions from the Co-operative Programme for Monitoring and Evaluation of the Long-range Transmission of Air Pollutants in Europe (EMEP) model [*Simpson et al.*, 2003].

2. Data and Methods

2.1. Satellite Data

[7] Data from the SCIAMACHY sensor onboard of the European Space Agency's Envisat platform was used for the purposes of this project as it currently provides the longest single-sensor time series of NO_2. SCIAMACHY is a hyperspectral UV/VIS/NIR passive imaging grating spectrometer observing the wavelength range of 214–2386 nm [*Bovensmann et al.*, 1999; *Gottwald et al.*, 2006]. Its overpass time is approximately 10:00 LST at the equator. Monthly averaged SCIAMACHY NO_2 data were obtained

from the Tropospheric Emission Monitoring Internet Service (TEMIS) web site. The NO_2 product is based on a combined retrieval and modeling approach developed at the Royal Netherlands Meteorological Institute (KNMI).

[8] In short, the NO_2 retrieval is based on three steps: The first step of the algorithm consists of a Differential Optical Absorption Spectroscopy (DOAS) retrieval of the total slant column of NO_2 from the measured spectrum, where absorption cross sections of NO_2, ozone, H_2O as well as a synthetic ring spectrum are taken into account, and a fifth order polynomial is included in the fit to account for scattering effects.

[9] The second step consists of the separation of the stratospheric and tropospheric NO_2 contributions to the total NO_2 column, where the stratospheric NO_2 column is estimated by assimilating total slant columns in the TM4 chemistry transport model [*Dentener et al.*, 2003; *Boersma et al.*, 2007]. The third and final step of the retrieval is the conversion of the tropospheric NO_2 slant columns into vertical columns using a calculated Air-Mass Factor (AMF). Further details on the specific retrieval methodology can be found in *Boersma et al.* [2004, 2007, 2011], as well as on the TEMIS web site (www.temis.nl). Solely data reprocessed with version 2.0 of the retrieval algorithm was used. Improvements in version 2.0 over previous versions of the retrieval algorithm include an updated albedo database, a modified calculation of the air mass factor, a correction of the surface height calculation, a correction of the weekly cycle in NO_x emissions, as well as an increased number of NO_x tracers in the applied chemical transport model [*Boersma et al.*, 2011]. The NO_2 data set used here only considered cloud radiance fractions of less than 50%. It was also resampled from the original SCIAMACHY spatial resolution to a 0.25×0.25 degree grid. For this study, monthly data between August 2002 and August 2011 was available.

[10] Although the NO_2 data set used in this study is based to some extent on data assimilation using the TM4 model [*Dentener et al.*, 2003; *Boersma et al.*, 2007], it is almost independent of the used emission inventory due to the retrieval set-up. The data assimilation results are mainly used to provide the stratospheric NO_2 column in the second step. This stratospheric column is virtually independent of the used emission database. For the calculation of the AMF in the third step knowledge of the profile shape of the vertical NO_2 distribution is needed. This profile shape is also taken from the data assimilation. However, the profile shape is independent of the emissions, since the data assimilation is scaling the NO_2 column with conservation of the shape. In conclusion, the NO_2 data are considered as retrieval results independent of emission data.

2.2. Trend Analysis

[11] In order to compute trends from the satellite data we follow the methodology suggested by *Weatherhead et al.* [1998] and later applied by *van der A et al.* [2006], *Good et al.* [2007], and *van der A et al.* [2008] for fitting a seasonal signal and a linear trend to monthly data. The monthly average NO_2 tropospheric column C_t at time t (in months) was thus modeled as

$$C_t = \mu + S_t + \frac{1}{12}\omega t + R_t \qquad (1)$$

where μ is a constant, S_t is a seasonal component, ω is a linear trend and R_t is the residual variability. The seasonal component S_t is modeled as

$$S_t = \sum_{j=1}^{4} \left[\beta_{1,j} \sin\left(\frac{2\pi jt}{12}\right) + \beta_{2,j} \cos\left(\frac{2\pi jt}{12}\right) \right] \qquad (2)$$

where $\beta_{1,1}$ through $\beta_{2,4}$ are coefficients of the fit. The residual variability R_t is assumed to be autoregressive of order 1 and was modeled as

$$R_t = \phi R_{t-1} + \epsilon_t \qquad (3)$$

where ϕ is the first order autocorrelation and ϵ is a random error component.

[12] The significance of the trend [*Santer et al.*, 2000] was computed based on the suggestion of *Tiao et al.* [1990] and *Weatherhead et al.* [1998] such that a trend ω is considered to be significant and to represent a real geophysical trend with a 95% confidence when $|\omega/\sigma_\omega| > t_\omega$, where σ_ω is the uncertainty of the trend and t_ω is the value of the Student's t-distribution for a significance level of $\alpha = 0.05$ and the degrees of freedom given for the time series [*Santer et al.*, 2000]. This approach slightly differs from previous studies, which assume a constant value of $t_\omega = 2$ [*Tiao et al.*, 1990; *Weatherhead et al.*, 1998; *van der A et al.*, 2006]. Finally, σ_ω is approximated according to *Weatherhead et al.* [1998] as

$$\sigma_\omega = \left[\frac{\sigma_r}{n^{3/2}} \sqrt{\frac{1+\phi}{1-\phi}} \right] \qquad (4)$$

where σ_r is the standard deviation of the de-trended residuals, n is the number of years with available data, and ϕ is the first-order autocorrelation. In order to eliminate spurious significant trends for time series with extremely low long-term averaged NO$_2$ column values $\overline{C}$ that are obviously below the uncertainty threshold of the satellite data (primarily over the oceans), the uncertainty for such time series was computed differently. If σ_ω as computed in Equation 4 was found to be less than a minimum uncertainty value of $\sigma_{min} = 0.65 + 0.3 \cdot \overline{C}$ [*Boersma et al.*, 2009] with $\overline{C}$ given in $\times 10^{15}$ molecules cm^{-2}, σ_ω was set equal to σ_{min}. In addition, trends were only computed for grid cells that exhibited a 9-year average of at least 1×10^{15} molecules cm^{-2}.

[13] Country averages were only computed when the satellite was able to provide data year-round, i.e. countries affected by polar night (Norway, Sweden, Iceland, and Finland) were not included in the analysis in order not to introduce a sampling bias for these countries. Furthermore a monthly country mean was only computed if at least 90% of the grid cells within the country boundaries exhibited valid NO$_2$ retrievals for this particular month. If trends are given for a specific place other than the country scale, unless otherwise noted the value was computed as the average trend over 3×3 grid cells centered over the coordinates of the location. Extreme outliers in the monthly data with a significance level of $\alpha < 0.001$ were eliminated from each time series prior to calculation of a trend using an iterative implementation of the Grubbs Test [*Grubbs*, 1969].

2.3. EMEP Data

[14] For a comparison of the satellite-derived NO$_2$ trends with model results, data from the Unified EMEP model was used. The model is described in detail in *Simpson et al.* [2003]. The data used was 1) gridded modeled tropospheric column of NO$_2$ for direct comparison with the satellite data 2) gridded modeled surface NO$_2$ concentrations and 3) gridded NO$_x$ emissions used as the input to the model. The data sets were obtained from the Meteorological Synthesizing Centre-West of EMEP (MSC-W) at the Norwegian Meteorological Institute.

[15] The EMEP model uses emissions collected by the Centre on Emission Inventories and Projections (CEIP) within the framework of the Co-operative program for monitoring and evaluation of long range transmission of air pollutants in Europe. A new emission inventory is produced every year at a 50 km by 50 km spatial resolution and is available at www.ceip.at. There are two versions of the inventory, one containing the official emissions as submitted by each party and one containing emissions that have been corrected and gap-filled. The latter version is used for running the EMEP model. More details on the emission inventory used for the EMEP model can be found in *Mareckova et al.* [2009].

[16] All data obtained from the EMEP model were available as gridded annual averages for the period 2002 to 2009. Data obtained from slightly different model versions had to be used for the approximately first and second half of the study period since no single model run covered the entire period. For the years 2002 to 2004 the Unified EMEP Model version 3.6 was used, whereas for the years 2005 to 2009 the EMEP/MSC-W Model version v2011-06 was used. A comparison during the overlap period of the two model versions (2005–2008) revealed no major differences with respect to spatial patterns in NO$_2$ except for a slight offset in values of the tropospheric NO$_2$ columns. The 2002–2004 version 3.6 NO$_2$ column data were corrected by this offset in order to make it match the data set used between 2005 and 2009. All EMEP data sets were provided in a gridded format at 50×50 km^2 horizontal resolution. For all comparisons with the EMEP model data, trends for SCIAMACHY NO$_2$ were recomputed specifically for the period August 2002 to December 2009 following the same methodology as described above. Note that the first 7 months of 2002 were not available for the satellite data set, however a closer investigation showed that this did not significantly alter the satellite trend over this period as it is based on monthly means rather than annual means. It was therefore decided to include the year 2002 in this analysis to achieve the maximum possible record length for comparison of the two data sets.

2.4. Station Data

[17] Europe-wide station observations of NO$_2$ were acquired from the European Air Quality Database (AirBase). Values of mean annual NO$_2$ concentration between 2002 and 2009 were available. Only background stations were considered for the purposes of this study. In addition, only stations with available data for all eight years of the study period were considered for computing station trends, thus resulting in a final number of 793 stations used. As the station data were available as annual means, the corresponding trends were computed using linear regression of the annual mean

values. Trends were also calculated non-parametrically using Sen's slope [*Sen*, 1968; *Gilbert*, 1987], yet the results of both methods were so similar that only the standard regression results are given. For all comparisons with the station data, trends for SCIAMACHY NO$_2$ were recomputed from monthly mean data specifically for the period August 2002 to December 2009 following the same methodology as described above.

3.   Results and Discussion

[18] In the following section we present the results of the study, which are roughly divided into three parts. The main focus lies in the spatial and temporal description of the trends found from SCIAMACHY for the August 2002 to August 2011 period. Global spatial patterns in trends are analyzed and trend values for the world's major megacities are given before the focus turns to Europe and a discussion of country-level average trends is given. Subsequently, these results are briefly compared to similar trends obtained from station data and from output of the EMEP model.

3.1.   Trends From SCIAMACHY

[19] The presentation of the results obtained from the trend analysis of the SCIAMACHY data is structured in two parts. First, major global patterns in NO$_2$ trends are analyzed. This is subsequently followed by a more detailed look at trends in Europe.

3.1.1.   Global Trend Patterns

[20] Figures 1 and 2 show the global patterns of trends derived from SCIAMACHY data between August 2002 and August 2011 in absolute and relative terms, respectively. Only trends statistically significant at the 95% level are shown. The most prominent feature is the area of strong NO$_2$ increase over eastern China. This phenomenon has been reported earlier utilizing primarily GOME data by *Richter et al.* [2005] and *van der A et al.* [2006]. Our study based solely on SCIAMACHY data finds large areas with significant trends exceeding 2×10^{15} molecules cm^{-2} yr^{-1} south of Beijing and northwest of Shanghai. These areas have been exhibiting significant growth and industrial development in recent years.

[21] Overall, the average of all significant trends over China between August 2002 and August 2011 was found to be 0.39 ($\pm$0.11) $\times 10^{15}$ molecules cm^{-2} yr^{-1} with a grid cell-level minimum of -1.45 ($\pm$0.44) $\times 10^{15}$ molecules cm^{-2} yr^{-1} and a grid cell-level maximum of 4.05 ($\pm$0.41) $\times 10^{15}$ molecules cm^{-2} yr^{-1}. This maximum, which is equal to an increase of 11.6 ($\pm$ 1.2) % yr^{-1}, was found over the city of Zibo (36.8°N, 118.0°E) in the Shandong province, a major transportation hub and industrial center.

[22] Figure 3 shows two time series of the mean monthly NO$_2$ concentrations over China, one for the mean of the entire area in China over which trends were computed, and one for only those areas that showed a statistically significant change (approximately 75% of the total area for which trends were computed). It further shows the associated linear trend components of the fitted statistical model. Both the annual cycle of NO$_2$ with a maximum in the months of December or January and an overarching linear trend are clearly visible in both time series. A dramatic increase in the annual range of NO$_2$ column values can also be observed, primarily expressed as an increase during the winter months.

[23] Figure 3 further shows the impact of the 2008/2009 global economic crisis on the Chinese economy. While China itself was not as severely affected as Europe and North America, the time series of average tropospheric NO$_2$ concentrations clearly shows that the peak levels during the 2008–2009 winter are significantly lower than the winter peak of the previous year, only reaching maximum levels of 7.4×10^{15} molecules cm^{-2} in December 2008 versus a value of 8.6×10^{15} molecules cm^{-2} reached in December 2007. While the effect of temporary emission reductions enforced during the 2008 Olympic games has been observed for NO$_2$ from space [*Mijling et al.*, 2009], the two time series shown in Figure 3 are computed over very large areas (34.5% and 45.9% of the total area of China, respectively), so that the impact of temporary emissions reductions carried out solely in the greater Beijing area can be considered negligible.

[24] The observed clear deviation from an otherwise rapidly increasing trend is therefore likely caused by a lowered demand from overseas and reduced emission levels of NO$_2$ from the industrial areas in China. However, a rapid recovery can be observed in the winter 2009/2010, when peak NO$_2$ concentrations again reached levels consistent with the previously observed increasing trend. Similar results identifying significant reductions of NO$_2$ over China between late 2008 and mid 2009 have been recently report by *Lin and McElroy* [2011] and attributed to the economic downturn. Using the GEOS-Chem model they found emission reductions of 20% from January 2008 to January 2009, which is very close to a reduction of 18% in thermal power generation during the same interval.

[25] Aside from the absolute values, the most rapid relative increase in NO$_2$ worldwide is also found in China, however in contrast to the hot spots mentioned previously it is located in an area of very low population density: A maximum of 19.8 ($\pm$1.9) % yr^{-1} was found at 25.4°N and 104.9°E. Also interesting is a large, consistent area of strong relative increase, centered around the city of Huolin Gol (45.52°N, 119.6°E) in the autonomous region of Inner Mongolia. Widespread increases between 15% yr^{-1} and 19% yr^{-1} were found in this area. The city's industry revolves primarily around coal production and power generation. Several major coal mines and coal power plants are located in the area. Coal production in China has been increasing in the last few decades and has done so quite rapidly with an average growth rate of 11.4% yr^{-1} between 1999 and 2009 and peak production not expected until around the year 2025 [*Lin and Liu*, 2010]. Related to these findings, *Zhang et al.* [2009] investigated the capability of OMI NO$_2$ data products for detecting new power plants or other large emitting facilities for a case study in the Inner Mongolia region in China. Figure 4 shows the relative trends in China in more detail.

[26] Two out of the three Chinese megacities listed in Table 1, namely Beijing and Shanghai, exhibit statistically significant positive NO$_2$ trends with values of 0.86 ($\pm$0.40) $\times 10^{15}$ molecules cm^{-2} yr^{-1} and 0.90 ($\pm$0.30) $\times 10^{15}$ molecules cm^{-2} yr^{-1}, respectively. Considering the associated uncertainties, these values are slightly lower than the results reported by *van der A et al.* [2006], who found trends of 1.2 ($\pm$0.5) $\times 10^{15}$ molecules cm^{-2} yr^{-1} for Beijing and 1.3 ($\pm$0.3) $\times 10^{15}$ molecules cm^{-2} yr^{-1} for Shanghai
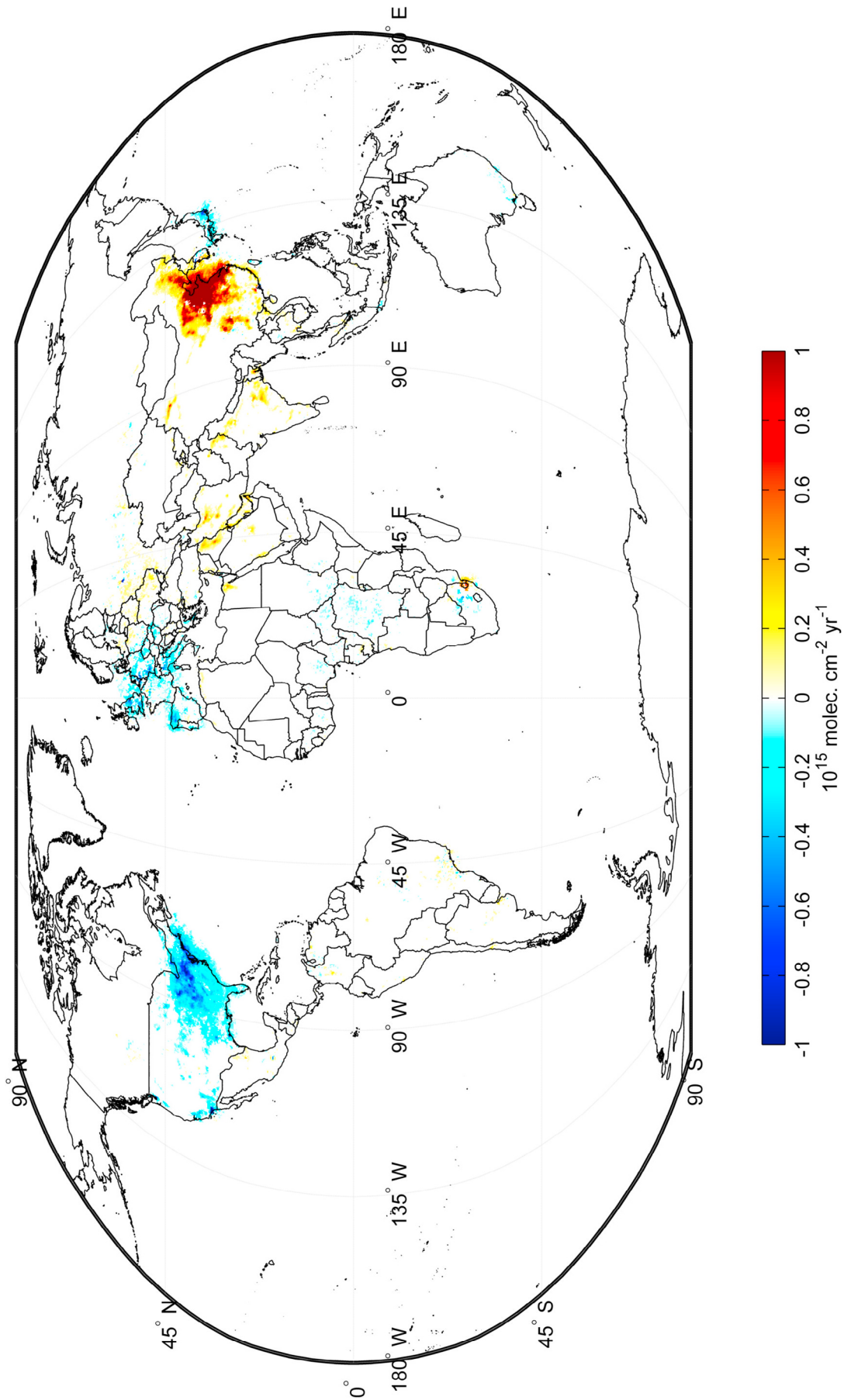
Figure 1. Absolute trends of tropospheric NO$_2$ concentration derived from SCIAMACHY data between August 2002 and August 2011. Units are given in $\times 10^{15}$ molecules cm^{-2} yr^{-1}. Only trends significant at the 95% level are being shown.
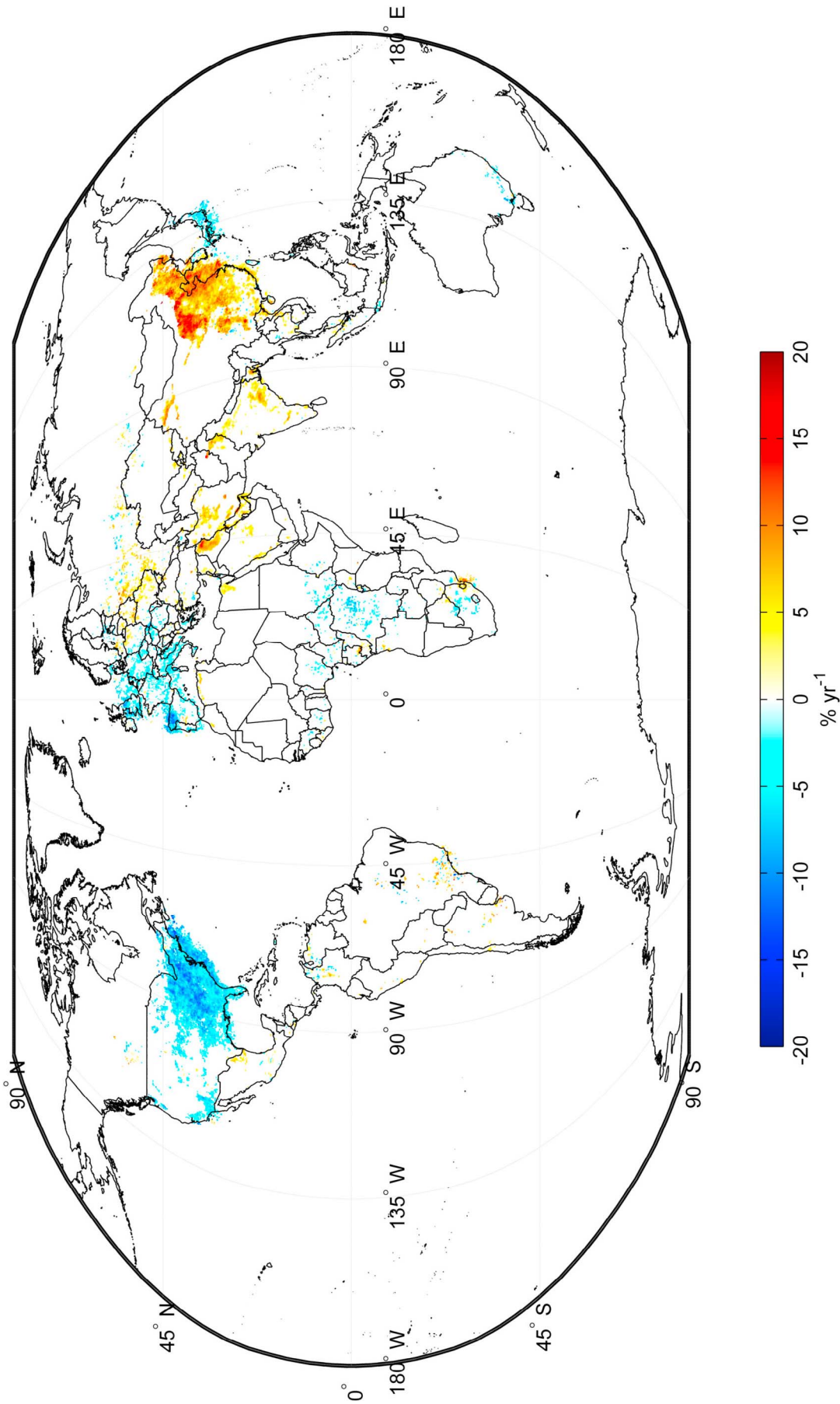
Figure 2. Relative trends of tropospheric NO$_2$ concentration derived from SCIAMACHY data between August 2002 and August 2011. Units are given in % yr^{-1}. Only trends significant at the 95% level are being shown. The absolute trend was normalized by the long-term mean value for each grid cell.
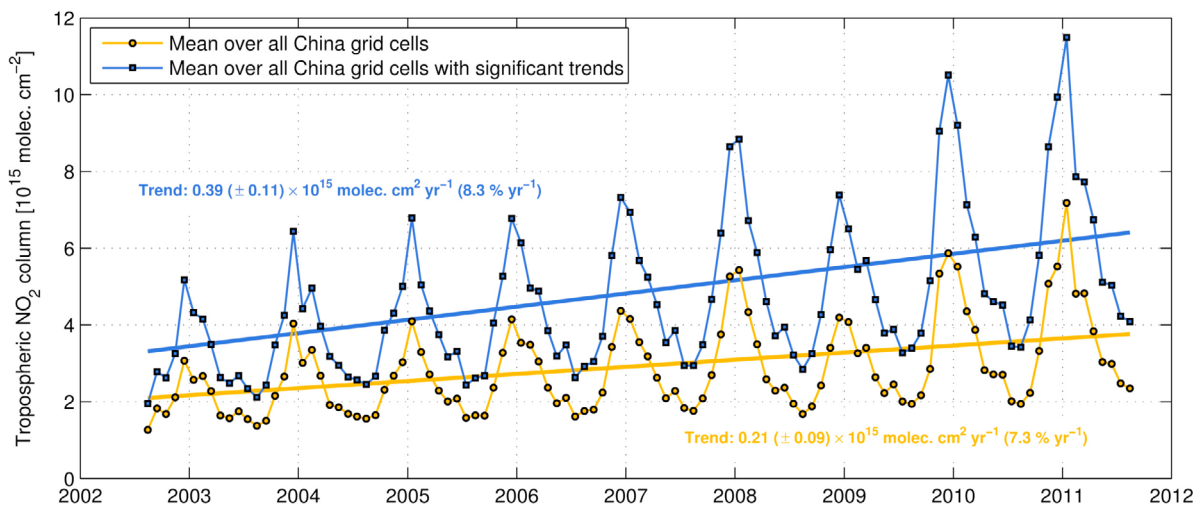
Figure 3. Time series of absolute mean monthly tropospheric NO_2 column over China. The figure shows average time series for all grid cells and for the grid cells with significant change only. The year label indicates the beginning of the respective year. The trends shown are the linear component of the fitted seasonal model. Relative trends are computed with respect to the 2002–2011 long-term average concentration.

between 1996 and 2006 using primarily GOME data. This indicates that the increase in NO_2 levels appears to have slowed down slightly in these regions. However, the trends in our study include the impact of the 2008/2009 global financial crisis which has possibly slightly reduced the longer-term magnitude of the trends.

[27] Strong increasing trends of NO_2 are further visible in Figures 1 and 2 over many large urban areas in southern Asia, primarily in India (2.7 ($\pm$1.5) % yr^{-1} in Delhi) and Bangladesh (9.5 ($\pm$1.7) % yr^{-1} in Dhaka), as well as in the Middle East, particularly in Iraq (9.5 ($\pm$1.6) % yr^{-1} in Baghdad), Iran (Kabul with a very rapid 16.1 ($\pm$2.1) % yr^{-1} albeit at a fairly low absolute value of 0.34 ($\pm$0.044) $\times 10^{15}$ molecules cm^{-2} yr^{-1}), and over the Persian Gulf. The only area in Asia with negative trends that are consistent over a spatially comparatively large region is Japan. Tokyo was found to have a quite rapid negative relative trend of -5.7 ($\pm$1.2) % yr^{-1}. Table 1 provides detailed trend values for several of these areas and other global megacities.

[28] With a few exceptions over some areas of Eastern Europe, both Europe and the United States generally exhibit widespread decreases in average tropospheric NO_2 concentrations. The strongest decreasing trends in Europe are found in the Po basin of Italy (-0.59($\pm$0.22) $\times 10^{15}$ molecules cm^{-2} yr^{-1}), the Stuttgart and Rhein/Ruhr urban agglomerations in Germany (-0.45($\pm$0.14) $\times 10^{15}$ molecules cm^{-2} yr^{-1} and -0.55 ($\pm$0.26) $\times 10^{15}$ molecules cm^{-2} yr^{-1}, respectively), and in the Northwest of Spain. Large areas of decreasing NO_2 levels can also be found over the United Kingdom. In the United States, statistically significant trends can be found primarily in the eastern half of the country with the strongest reductions of found south of the Great Lakes in the area of Ohio with relative decreases between -5% yr^{-1} and -10% yr^{-1} for the period 2002 to 2011. Similar results were reported by *Kim et al.* [2006], who found decreasing summertime trends of approximately -5% yr^{-1} between 1997 and 2005 in the Ohio River Valley, whose emissions are dominated by large power plants, thus indicating that the majority of reductions in this area are due to emission control measures. Further,

significantly decreasing trends were also found in the Los Angeles basin as well as the Central Valley and the Bay area of California. In contrast to *Kim et al.* [2009] we found a trend of approximately 5.1 ($\pm$1.4) % yr^{-1} for Los Angeles, whereas they found -2.53% yr^{-1} for the period 2003 through 2007. Discrepancies are likely due to the substantially longer time series used within our study. For San Francisco we found a significant trend of -6.7 ($\pm$1.6) % yr^{-1}, whereas *Kim et al.* [2009] report -8.13% yr^{-1} for the Bay area. It should be noted that not only different time periods but also varying areas for spatial averaging were used between these two studies, so quantitative comparisons should be made with caution. The significant decreases in tropospheric NO_2 in the United States are likely due to policy-driven emission reductions for power plants and the transport sector, with the dominant factor depending on region. To some extent, the economic recession starting in 2008/2009 affects the trends as well, as has been shown for Europe by *Castellanos and Boersma* [2012].

[29] Mostly weak and spatially non-consistent trends are also visible over small parts of South America and Central Africa. While the data over South America is known to be affected by increased noise levels due to the South Atlantic Anomaly (SAA) [*Heirtzler*, 2002] and therefore needs to be treated with caution, the slightly decreasing trends over central Africa could be associated to reduced biomass burning. Very similar weak trends over Africa were also found by *van der A et al.* [2008] when using combined GOME/SCIAMACHY data, however due to the very low overall NO_2 levels in the area and the noisy spatial patterns of the trends it is quite possible that other factors such as changes in cloud cover, surface albedo, aerosol, or meteorological conditions and not real decreases in NO_2 are the main reason for these trends [*van der A et al.*, 2006, 2008]. Further research using reliable in situ data will be required to determine the reality of such trends. One isolated area of significantly increasing trends is visible in the northeastern region of South Africa. This pattern is most likely associated with intensified use of coal power plants and mining activities in
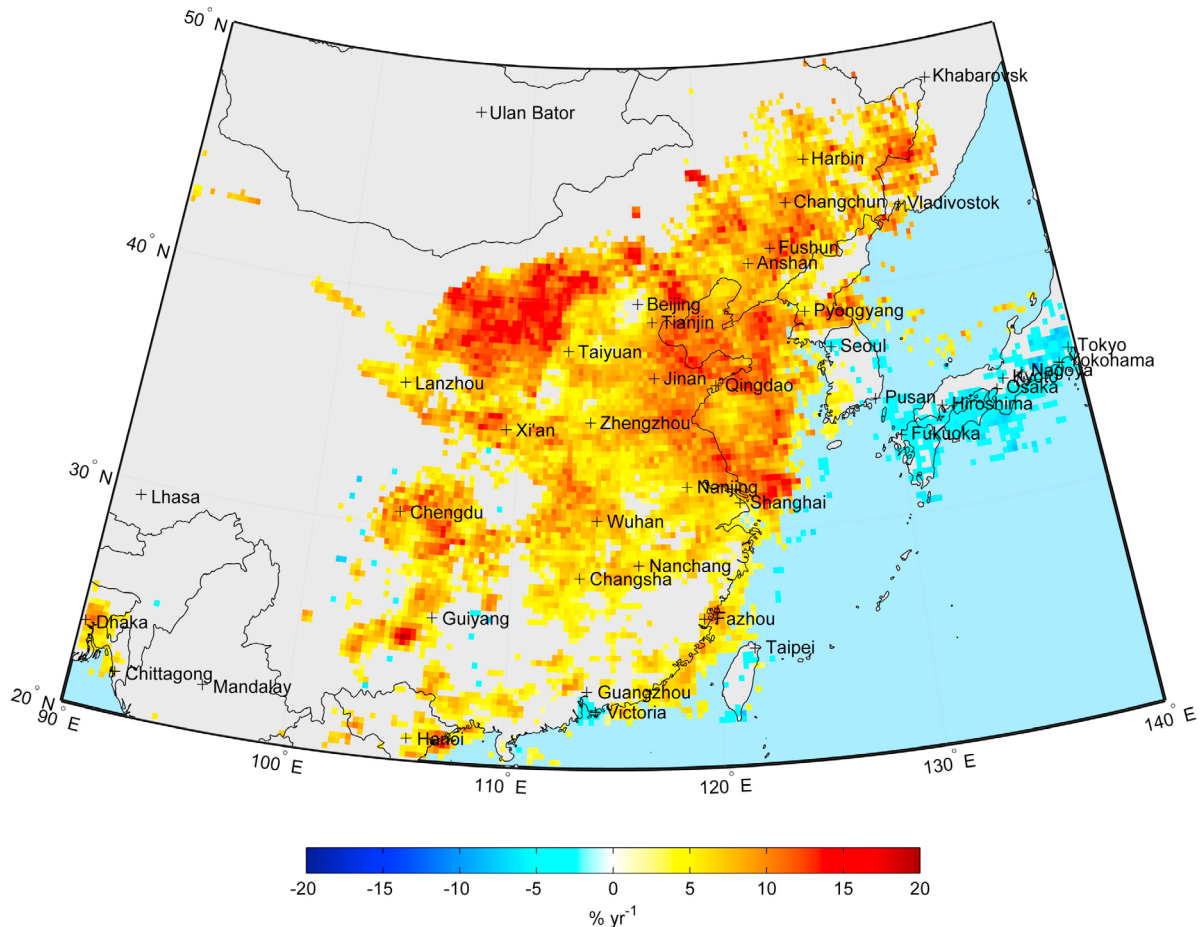
Figure 4. Relative trends of tropospheric NO$_2$ concentration in Eastern China. Trends were derived from SCIAMACHY data between August 2002 and August 2011. Units are given in % yr^{-1}. Only trends significant at the 95% level are being shown. The absolute trend was normalized by the long-term mean value for each grid cell.

the coal-rich regions of the Mpumalanga province of South Africa and in particular along the border to Swaziland [*Collett et al.*, 2010].

[30] The spatial patterns of tropospheric NO$_2$ trends found here confirm previous findings by *Richter et al.* [2005] and *van der A et al.* [2008]. While a quantitative comparison is challenging due to the different study periods and data sets used, the major spatial patterns of the trends, i.e. the rapidly increasing trends over Eastern China as well as decreasing trends over some areas of Europe and the Eastern part of the United States, remain consistent.

[31] In order to quantify trends for some of the most interesting areas, Table 1 provides both absolute and relative trend values in tropospheric NO$_2$ for the world's major megacities with a population of more than 10 million. 20 out of 27 sites exhibit trends which are statistically significant at the 95% confidence level. Eleven out of these 20 sites show increasing NO$_2$ levels and are nearly exclusively located in Asia and the Middle East (with the exception of Buenos Aires). The remaining 9 significant sites show decreasing trends. On an absolute level, Shanghai exhibits the most rapid increase in NO$_2$ with 0.90 ($\pm$0.30) $\times$ 10^{15} molecules cm^{-2} yr^{-1}, closely followed by Beijing with 0.90 ($\pm$0.30) $\times$ 10^{15} molecules cm^{-2} yr^{-1}. The megacity with the most rapid

relative increase is Dhaka in Bangladesh with a trend of 9.50 ($\pm$1.66) % yr^{-1}, closely followed by Baghdad with 9.37 ($\pm$1.56) % yr^{-1}. The most rapid decrease on the absolute scale was found for New York City with $-$0.98 ($\pm$0.24) $\times$ 10^{15} molecules cm^{-2} yr^{-1}, and for Tokyo on the relative scale with $-$5.74 ($\pm$1.25) % yr^{-1}.

3.1.2. Trends in Europe

[32] Focusing on temporal NO$_2$ variability in Europe, Figure 5 provides a more detailed map of the August 2002 to August 2011 trends from SCIAMACHY for the area, given in both absolute and relative units. At the absolute scale (Figures 5a and 5c), the majority of Europe exhibits negative trends, with the highest absolute decreases in NO$_2$ located around the agglomeration of the Ruhr area in Germany, the south of the Netherlands, and Belgium with values around $-$0.55 ($\pm$0.26) $\times$ 10^{15} molecules cm^{-2} yr^{-1}. The Stuttgart area also shows rapidly decreasing trends of $-$0.45 ($\pm$0.14) $\times$ 10^{15} molecules cm^{-2} yr^{-1}. Strong absolute decreases are also found over the Po basin in Italy ($-$0.51 ($\pm$0.19) $\times$ 10^{15} molecules cm^{-2} yr^{-1}), southern and central Great Britain (around $-$0.40 ($\pm$0.14) $\times$ 10^{15} molecules cm^{-2} yr^{-1}), as well as northwestern Spain. Large areas in Eastern Europe appear to indicate consistent patterns of slightly increasing NO$_2$ levels, however only small fractions of these trends are

Table 1. SCIAMACHY-Derived Tropospheric NO$_2$ Trends for Major Megacities Between August 2002 and August 2011[a]

City	N (months)	Absolute Trend (10^{15} molec. cm^{-2} yr^{-1})	Relative Trend (% yr^{-1})
Baghdad	107	**0.48 ± 0.08**	**9.37 ± 1.56**
Beijing	100	**0.86 ± 0.39**	**2.48 ± 1.14**
Buenos Aires	99	**0.20 ± 0.10**	**3.11 ± 1.61**
Cairo	109	**0.33 ± 0.11**	**4.59 ± 1.49**
Delhi	101	**0.20 ± 0.11**	**2.72 ± 1.45**
Dhaka	81	**0.45 ± 0.08**	**9.50 ± 1.66**
Guangzhou	77	−0.40 ± 0.31	−1.57 ± 1.22
Istanbul	97	0.01 ± 0.12	0.09 ± 1.44
Jakarta	83	**−0.21 ± 0.11**	**−2.63 ± 1.42**
Karachi	105	**0.09 ± 0.05**	**2.79 ± 1.63**
Kolkata	88	0.08 ± 0.07	2.10 ± 1.69
Lagos	55	**0.09 ± 0.05**	**3.68 ± 2.10**
London	91	**−0.44 ± 0.17**	**−3.30 ± 1.29**
Los Angeles	103	**−0.96 ± 0.26**	**−5.07 ± 1.36**
Manila	83	**−0.14 ± 0.08**	**−3.23 ± 1.82**
Mexico City	80	**−0.29 ± 0.19**	−1.67 ± 1.07
Mumbai	84	**0.14 ± 0.08**	**2.72 ± 1.48**
Moscow	74	−0.25 ± 0.24	−1.70 ± 1.63
New York	105	**−0.98 ± 0.24**	**−5.31 ± 1.29**
Osaka	81	**−0.35 ± 0.14**	**−2.59 ± 1.06**
Paris	95	**−0.37 ± 0.14**	**−3.30 ± 1.27**
Rio de Janeiro	62	0.05 ± 0.08	1.00 ± 1.53
Sao Paulo	85	−0.04 ± 0.13	−0.35 ± 1.16
Seoul	92	**−0.67 ± 0.30**	**−2.77 ± 1.23**
Shanghai	86	**0.90 ± 0.30**	**3.26 ± 1.07**
Tehran	103	**0.23 ± 0.13**	**2.19 ± 1.20**
Tokyo	99	**−1.23 ± 0.27**	**−5.74 ± 1.25**

[a]Numbers set in bold indicate a trend significant at the 95% confidence level. N indicates the number of months with valid data for each megacity. The trends were obtained for a 3 × 3 grid cell window (≈ 0.75 degrees × 0.75 degrees) located over the center of the city. The relative trend was obtained by normalizing the absolute trend using the long-term average NO$_2$ column for each location as a reference.

significant at the 95% confidence level. Such areas of significant trends are for example located in Northern Poland (0.09 (±0.05) × 10^{15} molecules cm^{-2} yr^{-1}), Southern Belarus (0.08 (±0.05) × 10^{15} molecules cm^{-2} yr^{-1}), and Eastern Ukraine (0.15 (±0.07) × 10^{15} molecules cm^{-2} yr^{-1}).

[33] The relative trends shown in Figures 5b and 5d indicate that several of the areas with very rapidly declining absolute concentrations are in fact fairly consistent with the surrounding areas when normalized by the mean level of NO$_2$ and are in the range between −1% yr^{-1} and −4% yr^{-1}. However, two spatially contiguous areas of rapidly decreasing NO$_2$ levels still appear in the map of relative trends and exceed such rates, namely central Great Britain in the area of Manchester and Leeds (−5.4 (±1.3) % yr^{-1}), as well as the northwest of Spain (−9.3 (±1.3) % yr^{-1}). The strong absolute and relative reduction in NO$_2$ in the northwestern region of Spain is particularly interesting in that no large urban areas are located in the primarily affected provinces of Léon and Asturias. However, several major power plants are scattered throughout the area and it is likely that either DeNOx technology has been installed there in recent years in response to policy-driven emission controls or that the impact of the economic crisis was particularly strong in this region and has led to substantially reduced NO$_2$ concentrations. These results have also been found very recently by *Zhou et al.* [2012] and *Castellanos and Boersma* [2012]. The areas of significant relative NO$_2$ increases are mostly scattered throughout eastern Europe. The only areas with spatially

contiguous increases appear to be northern Poland (3.9 (±1.9) % yr^{-1}), eastern Ukraine (3.2 (±1.5) % yr^{-1}), and western Russia (4.2 (±2.2) % yr^{-1}).

[34] Table 2 lists NO$_2$ trends derived from SCIAMACHY between August 2002 and August 2011 aggregated by country. As expected, the majority of European countries (27 out of 32) exhibit a negative trend in the NO$_2$ column concentration during this period. Five countries show a non-significant positive trend. All statistically significant trends are negative and are found in 7 countries overall (Germany, Hungary, Ireland, Italy, Netherlands, Slovenia, and the United Kingdom). No positive trends were found to be statistically significant. The most rapid and significant absolute mean trend was found for the Netherlands with a value of −0.40 (±0.12) × 10^{15} molecules cm^{-2} yr^{-1}, followed by the United Kingdom (−0.21 (±0.05) × 10^{15} molecules cm^{-2} yr^{-1}) and Germany (−0.20 (±0.1) × 10^{15} molecules cm^{-2} yr^{-1}). However, on a relative scale, Ireland shows the strongest significant decrease with a value of −4.5 (±2.3) % yr^{-1}, closely followed by the United Kingdom with −4.4 (±1.1) % yr^{-1} and the Netherlands with −4.2 (±1.2) % yr^{-1}. Weighted equally, the overall average relative trend among all studied countries was found to be −1.94% yr^{-1}. When computed as the trend of the mean monthly NO$_2$ value averaged over the entire study site, this value was found to be −2.0 (±2.3) % yr^{-1}.

[35] Table 2 further indicates the range of trend values found on a per-pixel level for each country. The most rapid negative per-pixel trend found was −0.88 (±0.25) × 10^{15} molecules cm^{-2} yr^{-1} and occurred in the Rhein-Ruhr area of Germany at approximately 51.4°N and 6.6°E. The most rapid positive per-pixel trend was found to be 0.20 (±0.09) × 10^{15} molecules cm^{-2} yr^{-1} and was located at approximately 49.6°N and 2.1°E in northern France. This significant trend was found in an area of two contiguous grid cells which are centered over the town of Beauvais. The trend is likely associated with the exceptionally rapid growth of the airport Beauvais-Tillé, which has become a major destination for low-cost airlines serving Paris during the last decade. Passenger numbers at this airport have increased by nearly 400% from 777,000 passengers in 2002 to 3.6 million in 2011 [*Union des Aéroports Français*, 2012].

[36] Despite fundamental differences in methodology these results can be at least qualitatively compared to previous studies. While *Konovalov et al.* [2008] studied primarily NO$_x$ emissions estimated from satellite data (primarily GOME) using model inversion, they also provide data on tropospheric NO$_2$ columns and they are one of the few studies that also investigate trends aggregated on the per-country level and provide such data for several countries. A relative comparison of the NO$_2$ trends for several major European countries shows similar magnitudes of the trends despite the different study periods used (1996 to 2005 versus 2002 to 2011 in this study) as well as a different methodology.

[37] For Germany, *Konovalov et al.* [2008] found a trend of −3.7 (±0.7) % yr^{-1} whereas this study found a trend of −3.3 (±1.6) % yr^{-1}. For France, they reported a trend of −2.3 (±0.8) % yr^{-1} while this study found −2.4 (±1.9) % yr^{-1}. Slightly larger differences exist for example for Great Britain where *Konovalov et al.* [2008] found a quite rapid NO$_2$ column trend of −6.3 (±0.6) % yr^{-1}, whereas this study found a value of only −4.4 (±1.1) % yr^{-1}. Overall,
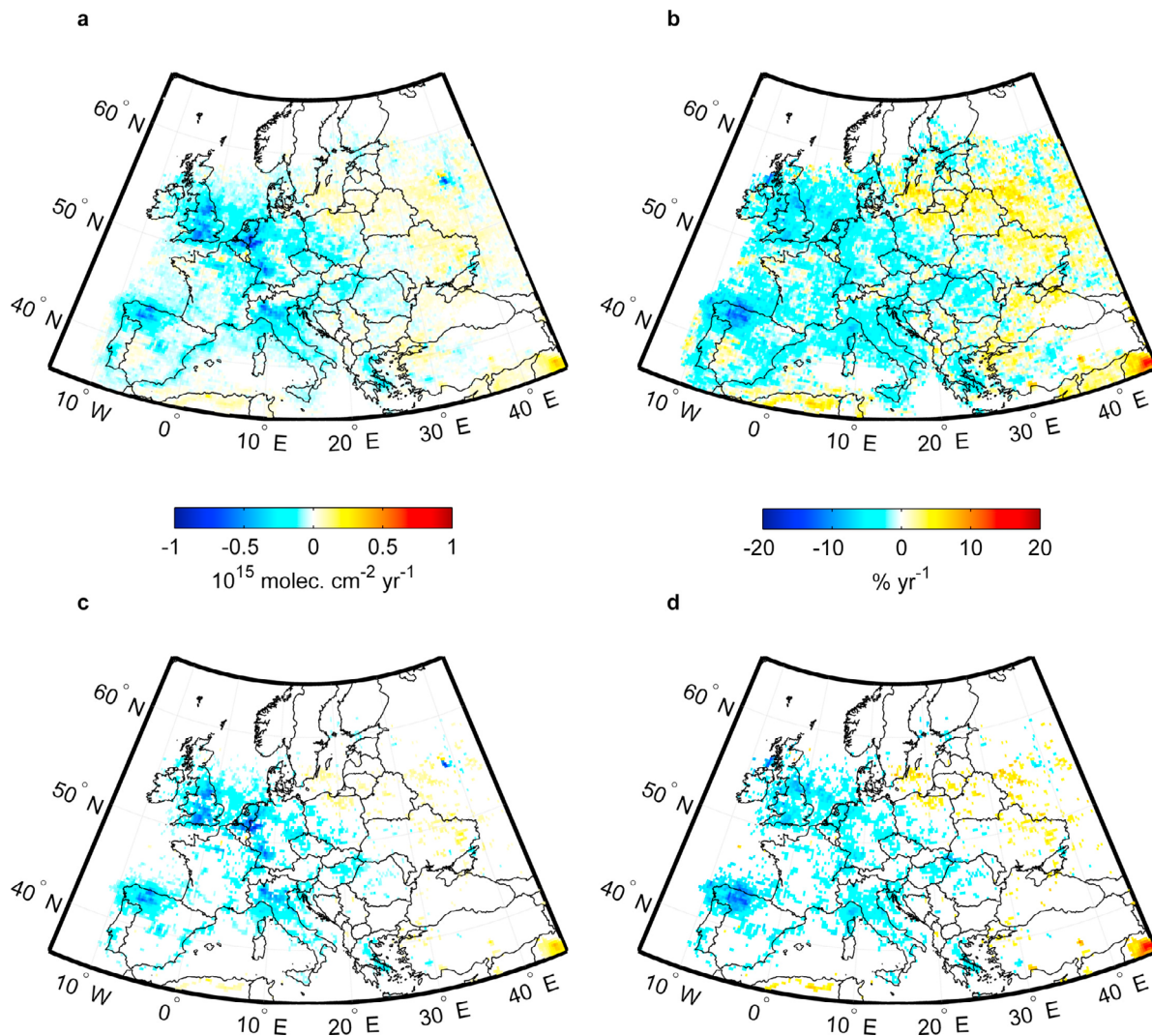
Figure 5. (a and c) Absolute and (b and d) relative trends of tropospheric NO$_2$ concentration over Europe. Figures 5a and 5b show all computed trends independent of their significance level whereas only trends significant at the 95% confidence level are shown in Figures 5c and 5d. The trends were derived from SCIAMACHY data between August 2002 and August 2011. Relative trends were computed by normalizing the absolute trends by the overall mean NO$_2$ level for each grid cell.

the magnitudes of the trends appear to be similar, though a detailed comparison is impossible due to the different methodologies used and the high uncertainties involved with each trend estimate. It should be noted that while the long-term decreasing trends in most of western Europe are primarily due to policy-driven NO$_x$ emission controls, the global economic downturn starting in 2008/2009 caused additional reductions, and the relationship between the two factors has been analyzed by *Castellanos and Boersma* [2012].

3.2. Comparison With Trends From Station Data

[38] In order to investigate to what extent the trends from SCIAMACHY-derived tropospheric NO$_2$ columns have the potential to be representative of trends from measurements taken at the ground level, the satellite-derived trends were compared with trends computed from station observations throughout Europe.

[39] Station-based studies of air quality trends have been carried out over Europe in the past. For example, *Guerreiro et al.* [2010] studied trends in European station observations of NO$_2$ and NO$_x$ between 1999 and 2008 and found a significant mean NO$_2$ trend for background stations of -0.28 μg m^{-3} yr^{-1} which is equivalent to -1.3% yr^{-1} during this period. While it is unlikely that such trends based on station observations can be reproduced exactly with the currently available satellite products of NO$_2$ due to vastly differing methodology and measurement scale, it is nonetheless valuable to investigate to what extent the two data sources agree. Only very few studies have attempted to compare satellite measurements of tropospheric NO$_2$ column with ground observations [*Petritoli et al.*, 2004; *Lamsal et al.*, 2010; *Blond et al.*, 2007], and to our knowledge trends from both data sources have never been directly compared. It should be noted here that directly comparing observations made by satellite with observations made by

Table 2. SCIAMACHY-Derived 2002–2011 NO$_2$ Trends Aggregated by Country[a]

Country	N (months)	Mean Abs. Trend (10^{15} molec. cm^{-2} yr^{-1})	Min. Abs. Trend (10^{15} molec. cm^{-2} yr^{-1})	Max. Abs. Trend (10^{15} molec. cm^{-2} yr^{-1})	Rel. Mean Trend (% yr^{-1})
Albania	90	−0.02 ± 0.05	**−0.08 ± 0.03**	**0.09 ± 0.04**	−1.65 ± 4.16
Austria	82	−0.02 ± 0.06	**−0.18 ± 0.10**	0.06 ± 0.05	−0.93 ± 2.48
Belarus	88	0.02 ± 0.04	−0.06 ± 0.05	**0.15 ± 0.05**	1.15 ± 2.38
Belgium	82	−0.20 ± 0.13	**−0.70 ± 0.21**	0.25 ± 0.14	−2.08 ± 1.31
Bosnia and Herz.	82	−0.03 ± 0.04	**−0.08 ± 0.04**	**0.10 ± 0.05**	−1.81 ± 2.79
Bulgaria	89	0.01 ± 0.05	−0.07 ± 0.05	**0.12 ± 0.05**	0.41 ± 2.74
Croatia	87	−0.08 ± 0.05	**−0.17 ± 0.05**	0.06 ± 0.06	−3.15 ± 2.00
Czech Republic	80	−0.11 ± 0.08	**−0.30 ± 0.11**	0.06 ± 0.07	−2.77 ± 2.21
Denmark	92	−0.07 ± 0.06	**−0.14 ± 0.07**	0.09 ± 0.06	−2.21 ± 1.91
Estonia	86	−0.01 ± 0.03	−0.09 ± 0.05	0.05 ± 0.04	−0.61 ± 2.70
France	85	−0.08 ± 0.06	**−0.52 ± 0.12**	**0.20 ± 0.09**	−2.44 ± 1.92
Germany	82	**−0.20 ± 0.10**	**−0.88 ± 0.25**	0.13 ± 0.11	**−3.29 ± 1.57**
Greece	100	−0.03 ± 0.05	**−0.38 ± 0.10**	**0.14 ± 0.06**	−1.70 ± 2.82
Hungary	86	**−0.10 ± 0.06**	**−0.26 ± 0.06**	0.10 ± 0.07	**−3.07 ± 1.84**
Ireland	78	**−0.09 ± 0.04**	**−0.22 ± 0.08**	0.10 ± 0.12	**−4.45 ± 2.29**
Italy	99	**−0.11 ± 0.06**	**−0.67 ± 0.25**	0.09 ± 0.10	**−3.00 ± 1.56**
Latvia	81	0.00 ± 0.04	−0.06 ± 0.04	**0.07 ± 0.04**	−0.36 ± 3.50
Lithuania	93	0.02 ± 0.04	−0.03 ± 0.04	**0.12 ± 0.04**	1.36 ± 2.72
Montenegro	82	0.00 ± 0.03	−0.04 ± 0.03	0.03 ± 0.03	0.53 ± 3.19
Netherlands	90	**−0.40 ± 0.12**	**−0.82 ± 0.16**	−0.06 ± 0.07	**−4.19 ± 1.24**
Poland	84	−0.05 ± 0.06	**−0.34 ± 0.13**	**0.20 ± 0.05**	−1.41 ± 1.77
Portugal	100	−0.05 ± 0.05	**−0.24 ± 0.09**	0.04 ± 0.04	−4.09 ± 3.63
Rep. of Moldova	90	0.00 ± 0.05	**−0.09 ± 0.04**	**0.08 ± 0.05**	0.02 ± 2.35
Romania	82	−0.03 ± 0.05	**−−0.15 ± 0.05**	**0.08 ± 0.05**	−1.50 ± 2.31
Serbia	82	−0.04 ± 0.05	−0.10 ± 0.06	**0.14 ± 0.08**	−1.70 ± 2.34
Slovakia	81	−0.07 ± 0.05	**−0.32 ± 0.05**	0.09 ± 0.08	−2.52 ± 1.81
Slovenia	89	**−0.10 ± 0.05**	**−0.22 ± 0.07**	0.04 ± 0.06	−2.96 ± 1.59
Spain	99	−0.08 ± 0.06	**−0.66 ± 0.10**	**0.07 ± 0.04**	−−3.80 ± 2.84
Switzerland	69	−0.10 ± 0.06	**−0.42 ± 0.13**	0.05 ± 0.04	−3.60 ± 2.27
Macedonia	91	−0.03 ± 0.05	**−0.10 ± 0.05**	0.06 ± 0.05	−1.44 ± 2.68
Ukraine	75	−0.01 ± 0.05	**−0.24 ± 0.06**	**0.20 ± 0.07**	−0.26 ± 2.17
United Kingdom	69	**−0.21 ± 0.05**	**−0.66 ± 0.14**	**0.14 ± 0.03**	**−4.44 ± 1.14**
Average	86	−0.07	—	—	−1.94

[a]Only European countries with an area of at least 5000 km^2 and a maximum latitude of 65°N were considered (see Section 2.2 for details). Numbers set in bold indicate a trend significant at the 95% confidence level. N indicates the number of months with valid data for each country. Min. Abs. Trend and Max. Abs. Trend indicate the range of trends found at the per-pixel level for each country.

ground stations is very challenging due to extreme differences in spatial scale of the observations, temporal sampling, and are particularly complicated by the fact that the satellite retrievals give measurements over the entire troposphere and are not very sensitive toward the Earth surface, where station observations are being made.

[40] Figure 6 provides a comparison of relative trends between 2002 and 2009 derived from monthly SCIAMACHY tropospheric NO$_2$ columns with trends obtained from mean annual station observations of NO$_2$ for the same period. For clarity, only stations with statistically significant trends are shown. The vast majority of stations are located in Germany and France and exhibit negative trends of the same magnitude as those obtained from SCIAMACHY for the same areas. In general, the spatial patterns in trends appear to agree between the two data sources. A few individual stations stand out as having quite different trends than the satellite data. In several such cases, these stations are surrounded by neighbors that do not indicate such extreme trends. It is thus reasonable to assume that these cases are outliers with respect to the larger scale trends and are likely to be subject to very local changes rather than to regional factors. Furthermore it should be noted that discrepancies in trends between satellite and in situ stations might also be caused by measurement issues and possibly inadequate quality control of the station data set.

[41] While the majority of stations exhibit negative trends, in the west of Spain the satellite data indicated an area of NO$_2$ increase and a cluster of three stations in the area ("Salamanca 4", "Cáceres", and "Monfragüe") is consistent with that trend. On the other hand, several stations located at the coast of Portugal also indicate slightly increasing trends, yet the satellite data does not show this pattern.

[42] The vast majority of stations exhibits negative NO$_2$ trends. A total of 626 out of 793 stations showed a negative trend whereas the satellite data indicated a negative trend at 697 station locations. Computed over all 793 suitable stations, the overall mean trend was found to be −0.34 μg m^{-3} yr^{-1} or −1.65% yr^{-1}. This is slightly more rapid than a corresponding trend of −0.28 μg m^{-3} yr^{-1} or −1.3% yr^{-1} found by *Guerreiro et al.* [2010], who used a different subset of the same data set. The mean relative SCIAMACHY trend over the same locations was found to be −3.02% yr^{-1} with a standard deviation of 2.59% yr^{-1}. The situation improves significantly when only stations with a statistically significant trend (at the 95% confidence level) are considered. In this case the mean station trend is −3.33% yr^{-1} with a standard deviation of 3.29% yr^{-1} whereas the mean relative satellite trend at the station locations is −3.15% yr^{-1} with a standard deviation of 2.6% yr^{-1}.
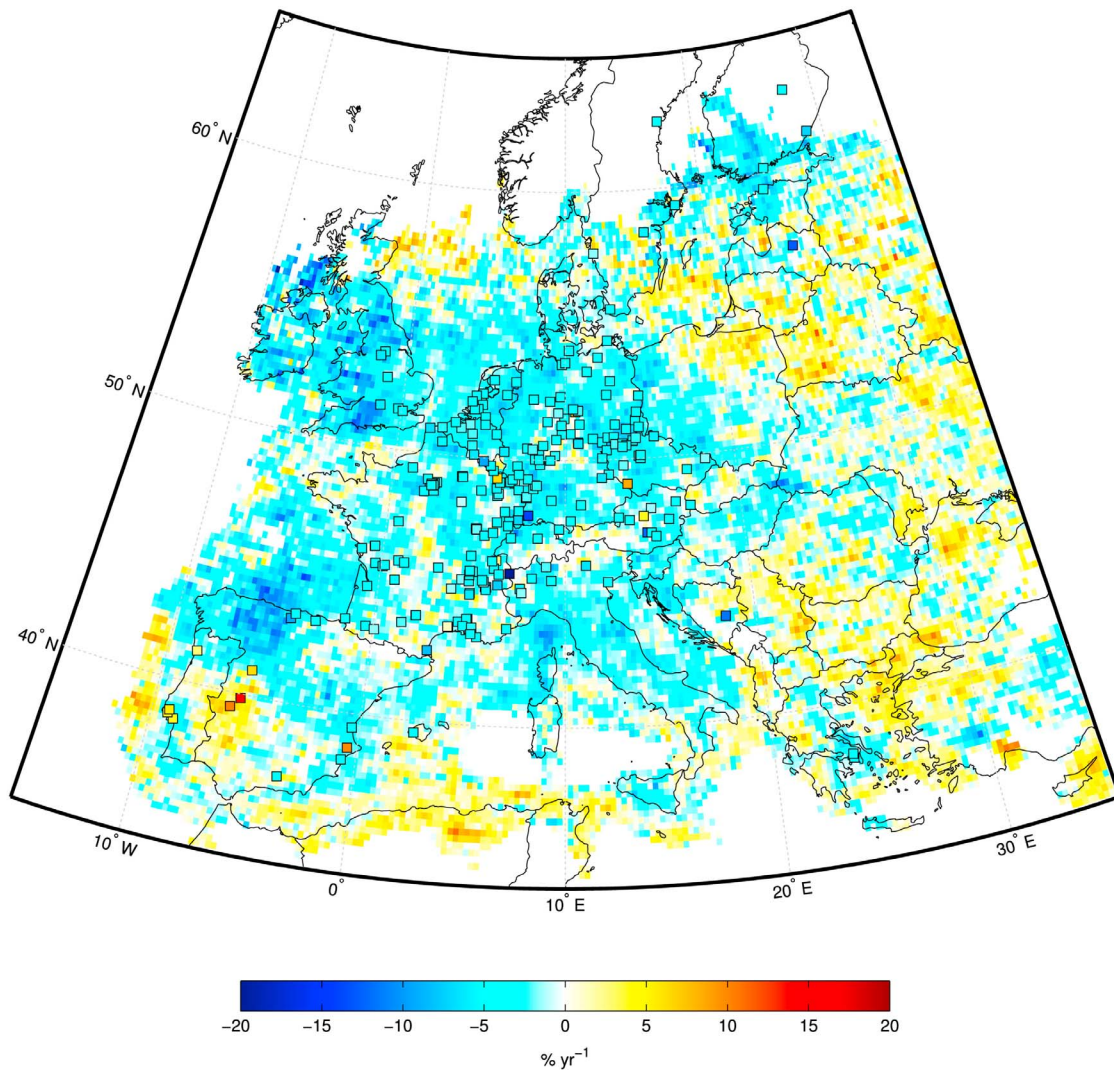
Figure 6. Comparison of relative 2002–2009 NO₂ trends derived from SCIAMACHY with NO₂ trends obtained from Airbase station data over Europe for the period 2002 to 2009. SCIAMACHY trends are plotted in the background whereas station trends are shown as squares with the color of the square indicating the trend measured at the station. For clarity, all available satellite trends but only stations with statistically significant trends at the $p < 0.05$ level are shown. The same color scale is used for both data sets. Note that satellite trends were only computed in areas with a mean concentration greater than 1×10^{15} molecules cm^{-2}.

[43] While this result is encouraging, aggregating this information on the country level reveals larger differences. Table 3 shows a comparison of station-based relative NO₂ trends with SCIAMACHY-derived relative NO₂ trends aggregated on a per-country level for the period 2002 to 2009. The country averages were only computed for countries that had a minimum number of 10 stations with full temporal data coverage. While in all cases the trends derived from the two data sources agree in sign, the quantitative agreement between the two data sources is quite variable. In the majority of cases the difference between satellite and station trends is less than 2% yr^{-1}, however in some cases the difference was found to be exceeding 3% yr^{-1}, such as for the United Kingdom. This difference in trend can be explained by the fact that most

stations are located in England and not in Scotland where the air is quite clean. In other cases, such as for Austria or Poland, the trends from the two data sources are very close. On average, the SCIAMACHY trend found at the station locations was −2.9% yr^{-1} whereas the mean trend of country averages was found to be −1.3% yr^{-1}. The latter trend of −1.3% yr^{-1} is consistent with the one found by *Guerreiro et al.* [2010] using a different subset of the same data set. Overall, the mean difference for all countries listed in Table 3 was found to be −1.5% yr^{-1}.

[44] These results indicate that there appears to be a consistent offset in terms of relative NO₂ surface trends at the stations and tropospheric NO₂ columns measured by the satellite - at least when station with both significant and non-

Table 3. Country-Level Averages of Relative NO_2 Trends Between 2002 and 2009 From Both SCIAMACHY and Station Observations[a]

Country	N	Satellite (Entire Country) (% yr^{-1})	Satellite (at Stations) (% yr^{-1})	Stations (% yr^{-1})	Difference (% yr^{-1})
Austria	71	-1.2 ± 3.5	-1.7 ± 2.6	-1.1 ± 0.7	-0.6
Belgium	19	-4.2 ± 1.6	-4.0 ± 1.9	-2.1 ± 0.6	-1.9
Czech Republic	35	-3.9 ± 3.0	-3.5 ± 2.3	-2.0 ± 0.7	-1.5
France	255	-2.7 ± 2.7	-3.0 ± 2.4	-1.9 ± 0.7	-1.0
Germany	183	-4.1 ± 2.1	-4.0 ± 2.2	-1.7 ± 0.6	-2.3
Italy	33	-3.0 ± 2.0	-2.1 ± 2.2	-0.6 ± 0.6	-1.4
Netherlands	26	-5.2 ± 1.7	-3.8 ± 1.9	-2.1 ± 0.8	1.7
Poland	11	-2.4 ± 2.4	-0.1 ± 2.3	-0.1 ± 0.9	0.0
Spain	58	-3.0 ± 3.3	-2.1 ± 2.6	-1.2 ± 0.7	-0.9
Switzerland	22	-3.8 ± 3.2	-3.2 ± 2.5	-1.4 ± 0.7	-1.7
United Kingdom	22	-4.9 ± 1.6	-4.5 ± 2.3	-0.6 ± 0.7	-3.9
Average	67	-3.5	-2.9	-1.3	-1.5

[a]Averages were only computed for countries that had a minimum number of 10 qualifying stations. Note that the computed uncertainty values of satellite trends are generally higher due to the shortened study period. The difference was computed as the satellite trend averaged over the station locations minus the average station trend for each country.

significant trends are considered. This discrepancy could be caused by several reasons: Unfortunately, a common overlap period of only seven years of data was available from both data sets. Thus, the trends that were computed over this period are subject to a higher uncertainty than the 2002 to 2011 trends computed above, thus complicating the comparison of the two data sets in addition to vastly different methodologies.

[45] Furthermore, retrievals of NO_2 are only obtained during cloud-free atmospheres, and the entire satellite record therefore has a clear sky bias, causing possible effects particularly during generally more polluted winter months. The trends computed from both data sets are further based on observation at different times. Whereas the satellite observations are made at approximately 10:00 local time, the trends obtained from the stations are based on regularly sampled averages. More research using significantly longer time series and looking particularly at specific reason for this bias will be necessary to validate these results and to draw further conclusions. It should be noted in addition that comparing country-wide trends from station and satellite observations is further complicated by the spatial coverage of each measurement type. While station observations, which are generally highly accurate, are only representative of their immediate surroundings and therefore many areas are not considered when computing a country-wide average, satellite data allows for a spatially continuous measurement for the entire country albeit at the expense of a higher measurement uncertainty.

3.3. Comparison With Trends From the EMEP Model

[46] The EMEP emission inventory [*Vestreng et al.*, 2005] and the output from the unified EMEP model [*Simpson et al.*, 2003] has been used in the past with respect to trend analysis. For example, *Konovalov et al.* [2008, 2010] used data from the EMEP emission inventory for comparing them to satellite-derived trends in NO_x emissions. *Fagerli and Aas* [2008] studied station observations of long-term trends for several nitrogen compounds and compared them with results from the EMEP model, however they did not study trends in NO_2 concentration specifically. *Vestreng et al.* [2009] studied long-term trends in NO_x emissions in Europe based partly on EMEP emission inventories.

[47] In order to estimate the model's capabilities with respect to correctly predicting magnitude and in particular spatial patterns of trends of NO_2 in the atmosphere, a simple comparison was carried out. During the period for which adequate data from both data sources was available (2002–2009), trends were computed from the SCIAMACHY data using the methodology explained above and subsequently compared with corresponding trends obtained from the output of the EMEP model, in particular from data on tropospheric column trends as well as surface NO_2 trends. Furthermore trends in NO_x emission estimates used for the EMEP model were also computed and compared.

[48] While a comparative trend analysis does not necessarily require two data sources to agree at an absolute level but only in terms of the magnitude of temporal change, it is nonetheless informative to investigate to what extent the EMEP model is able to recreate the absolute tropospheric NO_2 columns as observed by SCIAMACHY. For this purpose, 2005–2009 average tropospheric NO_2 column maps were derived from both sources and compared. Figure 7 shows the results. Qualitatively there is a good agreement in terms of general spatial patterns. The large area of high NO_2 concentrations in the Po basin of Italy as well as most major metropolitan areas are well replicated by the model. In particular the three hot spots in Western Germany, the Netherlands, and Belgium are visible in both data sources. However, it is also clear from a simple visual analysis of Figure 7 that the absolute values obtained from the model are overall higher than those observed by SCIAMACHY. This is particularly noticeable over Germany where the model indicates values around 8×10^{15} molecules cm^{-2} yr^{-1} throughout most of the country, whereas the satellite instrument observes such concentrations only over the more densely populated areas.

[49] It should be noted, that the satellite observations made by SCIAMACHY occur at approximately 10:00 local time, whereas the EMEP model was run continuously and regularly sampled and then averaged. Given the significant diurnal cycle of NO_2 a direct quantitative comparison of these two data set is therefore not very meaningful. A sampling of the model solely at the satellite overpass times would be preferable for this purpose but was not possible in this study due to the lack of hourly model data.
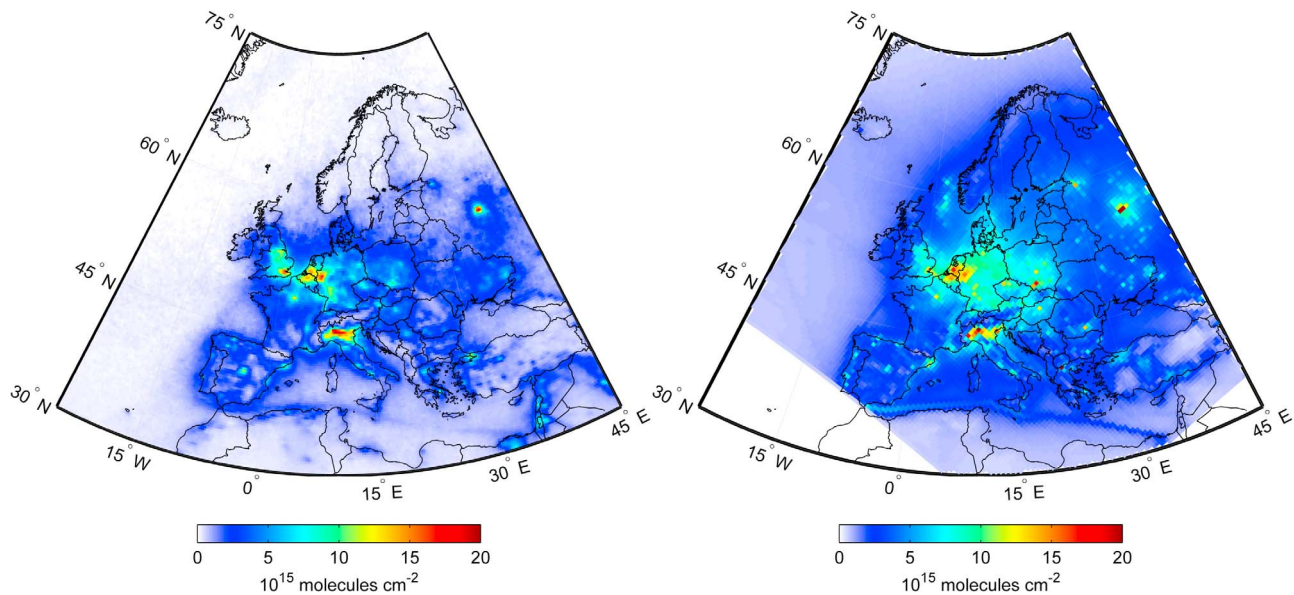
Figure 7. Average tropospheric NO_2 column for the years 2005 to 2009 (left) derived from SCIAMACHY and (right) modeled using the EMEP model. Note that SCIAMACHY columns were observed only at approximately 10:00 local time, whereas the EMEP model was run continuously and sampled regularly.

[50] The annual mean derived from the SCIAMACHY instrument might further be biased slightly low due to the necessity for clear-sky conditions for obtaining valid retrievals. Since SCIAMACHY might capture fewer of the NO_2 peaks during the winter months due to increased cloud cover in that period, its monthly mean estimates might be slightly low. However, since the annual mean was computed from monthly mean values weighting all months equally, the bias should be reasonably small, as opposed to computing the annual mean from averaging daily values, where the bias could be more substantial.

[51] Nonetheless, given that the NO_2 columns derived from the model mostly agree with the SCIAMACHY NO_2 columns in terms of spatial patterns, it is interesting to investigate if the model is still able to simulate similar trends in NO_2 levels as is shown by the satellite. Figure 8 shows a comparison for the period 2002 to 2009 of tropospheric column NO_2 trends obtained from SCIAMACHY with trends in EMEP model output, in particular with modeled tropospheric NO_2 column, modeled surface NO_2 concentration, as well as trends in NO_x emissions used in the EMEP model. The SCIAMACHY-derived spatial patterns in trends computed for the period 2002 to 2009 (Figure 8a) are obviously similar to the trend maps derived for the full study period (see Figure 5), albeit they are associated with slightly higher uncertainties due to the shorter time series. A qualitative comparison with the model-derived trends in NO_2 columns (Figure 8b) shows relatively good agreement over central and western Europe. All the major areas of decreasing NO_2 levels, in particular over western Germany, the Netherlands, Belgium, northern Italy and the UK have been captured by the model. Furthermore the previously discussed area of rapid NO_2 decrease in the Spanish provinces of Léon and Asturias has been adequately reproduced by the model although the spatial patterns in trends appear more

localized than in the satellite-derived trend map. Over northern Italy and the east of Great Britain the model indicates slightly more rapidly declining NO_2 levels that have been observed by the satellite. The model has also been able to adequately replicate areas of small or no change in NO_2 column, such as over Austria, western and southern France, Scotland, Ireland, as well as large parts of the Iberian peninsula. The model further shows slightly increasing trends along the major shipping lanes in the Mediterranean which has been observed to some extent by the SCIAMACHY data as well.

[52] While the qualitative agreement over western and central Europe is encouraging, major differences between the trends from the two data sources can be observed throughout Eastern Europe. While SCIAMACHY has detected increasing trends in some parts of Eastern Europe, in particular over northern Poland, southern Belarus, eastern Ukraine and western Russia, the model-derived trends appear to be much more wide-spread throughout all of eastern Europe. The model further indicates very rapidly increasing trends in NO_2 column over the North Sea. These are not visible in the SCIAMACHY-derived trend map.

[53] As mentioned previously, two slightly different model versions had to be used to cover the entire 2002 to 2009 period and a small bias that was found between the two model versions with respect to mean NO_2 column concentration had to be corrected manually. This might have negatively impacted the model trends, and further research using a long and consistent model time series computed with the exact same model version will be required to draw any further conclusions.

[54] Figure 8c shows the trends in EMEP model output for surface NO_2 levels. While not directly comparable to the SCIAMACHY-derived trends, it is nonetheless interesting to investigate to which extent the spatial patterns in trend
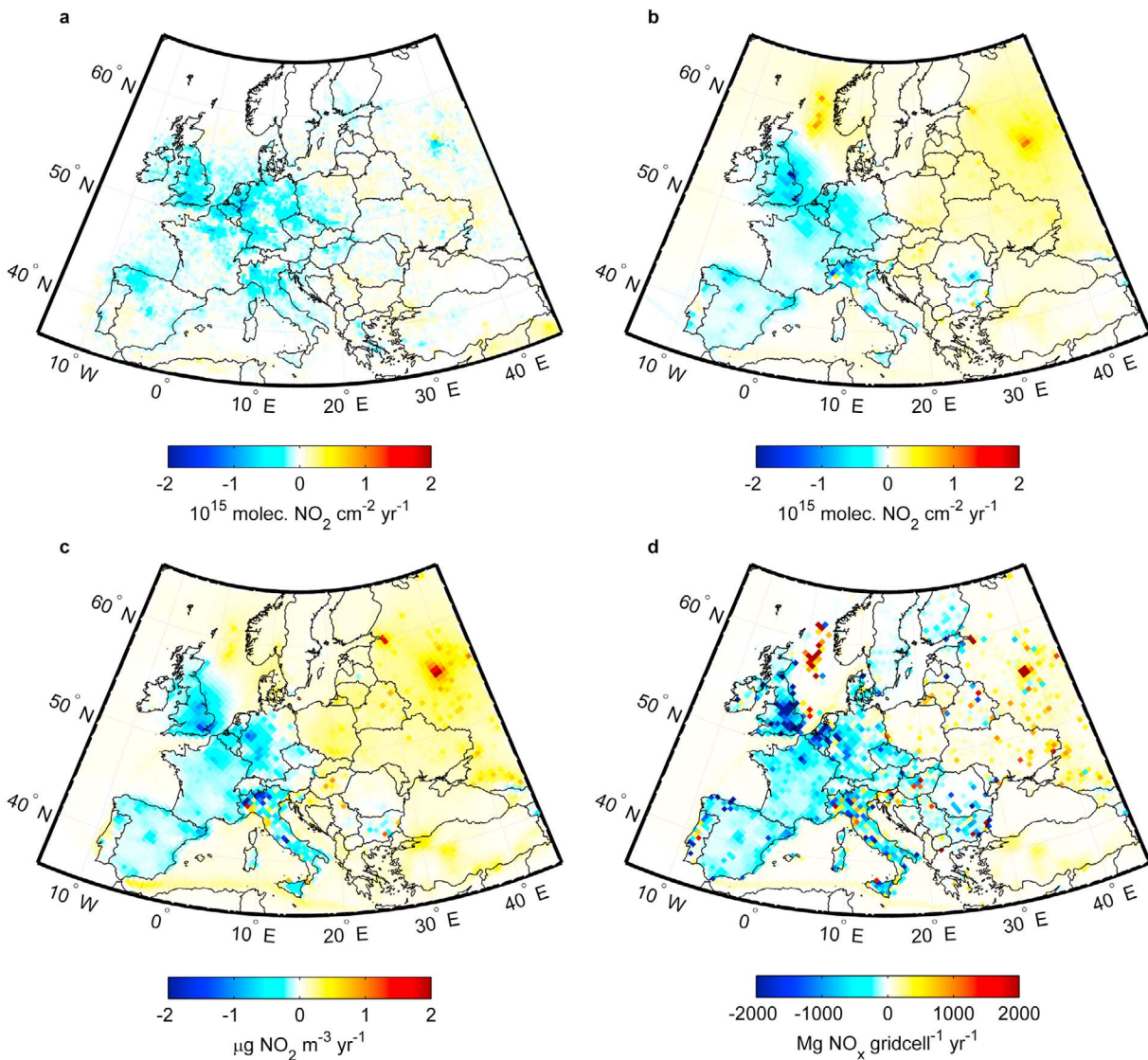
Figure 8. Comparison of 2002 to 2009 trends of (a) SCIAMACHY tropospheric column NO$_2$ with (b) EMEP-derived tropospheric column NO$_2$, (c) EMEP-derived surface NO$_2$, and (d) NO$_x$ emissions used in the EMEP model.

computed from both data sources agree. Again, the EMEP model output corresponds well to the SCIAMACHY trends in central and western Europe. The declining trends in NO$_2$ over western Germany, Belgium, Netherlands, and the United Kingdom are well replicated. Furthermore the slightly decreasing trends over large areas of France as well as in northern Spain are shown by the model output. The surface NO$_2$ trends are particularly rapid over northwestern Italy. This can also be seen to some extent in the NO$_2$ column data, but the satellite trends do not show such behavior.

[55] Finally, Figure 8d shows trends in NO$_x$ emissions that are used for the EMEP model. As expected, estimated NO$_x$ emissions have been declining over the majority of Europe with only small areas of increase, such as over the North Sea and a few isolated locations over eastern Europe.

[56] In order to quantify these results, Figure 9 shows a scatterplot comparing 2002–2009 country-level trends in tropospheric NO$_2$ column from both SCIAMACHY data and

EMEP model output. The trends derived from the EMEP model and from SCIAMACHY approximately follow the 1:1 line, thus indicating at least general correspondence. The EMEP model underestimates the trends for countries with more rapid decline in NO$_2$ levels of around -0.2×10^{15} molecules cm^{-2} yr^{-1} and tends to indicate slightly increasing trends when the SCIAMACHY data show no substantial trend in either direction. The trends from both data sources are correlated with a correlation coefficient of 0.79, a mean bias of 0.037×10^{15} molecules cm^{-2} yr^{-1} and an RMSE of 0.09×10^{15} molecules cm^{-2} yr^{-1}. The overestimation of the trends from the EMEP model for Eastern European countries can be clearly seen in Figure 9. For most of the countries that show a positive trend based on EMEP data, the satellite trends are around zero.

[57] These results indicate that despite substantial differences in absolute levels of NO$_2$, the EMEP model is capable of replicating spatial patterns in trends observed from space
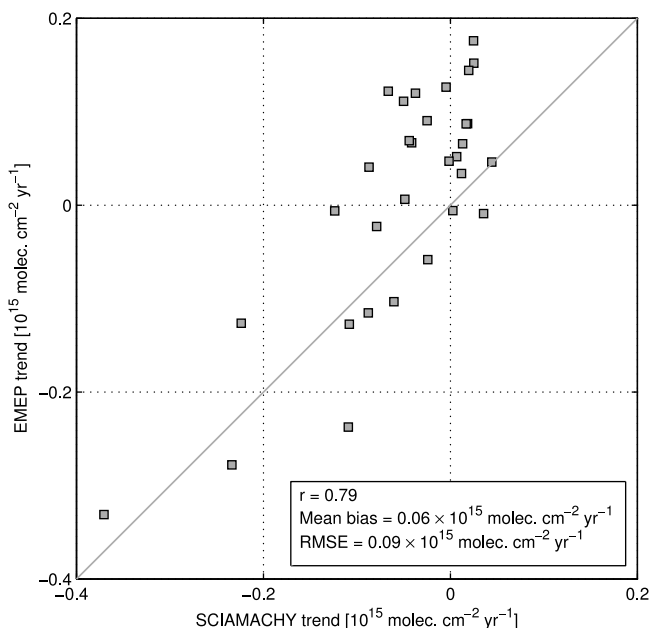
Figure 9. Scatterplot comparing 2002–2009 country-level trends in NO$_2$ column in Europe derived from SCIAMACHY and the unified EMEP model. The 1:1 line is indicated in gray.

and furthermore to derive country-level trends of tropospheric NO$_2$ column with a negligible bias of 0.037×10^{15} molecules cm^{-2} yr^{-1} and an RMSE of 0.09×10^{15} molecules cm^{-2} yr^{-1} with respect to SCIAMACHY trends.

References

Blond, N., K. F. Boersma, H. J. Eskes, R. J. van der A, M. Van Roozendael, I. De Smedt, G. Bergametti, and R. Vautard (2007), Intercomparison of SCIAMACHY nitrogen dioxide observations, in situ measurements and air quality modeling results over western Europe, *J. Geophys. Res.*, *112*, D10311, doi:10.1029/2006JD007277.

Boersma, K. F., H. F. Eskes, and E. J. Brinksma (2004), Error analysis for tropospheric NO$_2$ retrieval from space, *J. Geophys. Res.*, *109*, D04311, doi:10.1029/2003JD003962.

Boersma, K. F., et al. (2007), Near-real time retrieval of tropospheric NO$_2$ from OMI, *Atmos. Chem. Phys.*, *7*, 2103–2118.

Boersma, K. F., D. J. Jacob, M. Trainic, Y. Rudich, I. DeSmedt, R. Dirksen, and H. J. Eskes (2009), Validation of urban NO$_2$ concentrations and their diurnal and seasonal variations observed from the SCIAMACHY and OMI sensors using in situ surface measurements in Israeli cities, *Atmos. Chem. Phys.*, *9*(12), 3867–3879, doi:10.5194/acp-9-3867-2009.

Boersma, K. F., et al. (2011), An improved tropospheric NO$_2$ column retrieval algorithm for the Ozone Monitoring Instrument, *Atmos. Meas. Tech.*, *4*, 1905–1928, doi:10.5194/amtd-4-2329-2011.

Bovensmann, H., J. P. Burrows, M. Buchwitz, J. Frerick, S. Noël, V. V. Rozanov, K. V. Chance, and A. P. H. Goede (1999), SCIAMACHY: Mission objectives and measurement modes, *J. Atmos. Sci.*, *56*(2), 127–150, doi:10.1175/1520-0469(1999)056<0127:SMOAMM>2.0.CO;2.

Burrows, J. P., et al. (1999), The Global Ozone Monitoring Experiment (GOME): Mission concept and first scientific results, *J. Atmos. Sci.*, *56*(2), 151–175, doi:10.1175/1520-0469(1999)056<0151:TGOMEG>2.0.CO;2.

Castellanos, P., and K. F. Boersma (2012), Reductions in nitrogen oxides over Europe driven by environmental policy and economic recession, *Sci. Rep.*, *2*, 265, doi:10.1038/srep00265.

Collett, K. S., S. J. Piketh, and K. E. Ross (2010), An assessment of the atmospheric nitrogen budget on the South African Highveld, *S. Afr. J. Sci.*, *106*(5/6), 1–9, doi:10.4102/sajs.v106i5/6.220.

Dentener, F., M. van Weele, M. Krol, S. Houweling, and P. van Velthoven (2003), Trends and inter-annual variability of methane emissions derived from 1979–1993 global CTM simulations, *Atmos. Chem. Phys.*, *3*, 73–88.

Fagerli, H., and W. Aas (2008), Trends of nitrogen in air and precipitation: Model results and observations at EMEP sites in Europe, 1980–2003, *Environ. Pollut.*, *154*(3), 448–461, doi:10.1016/j.envpol.2008.01.024.

Ghude, S. D., S. Fadnavis, G. Beig, S. D. Polade, and R. J. van der A (2008), Detection of surface emission hot spots, trends, and seasonal cycle from satellite-retrieved NO$_2$ over India, *J. Geophys. Res.*, *113*, D20305, doi:10.1029/2007JD009615.

Ghude, S. D., R. J. Van der A, G. Beig, S. Fadnavis, and S. D. Polade (2009), Satellite derived trends in NO$_2$ over the major global hotspot regions during the past decade and their inter-comparison, *Environ. Pollut.*, *157*(6), 1873–1878, doi:10.1016/j.envpol.2009.01.013.

Gilbert, R. O. (1987), *Statistical Methods for Environmental Pollution Monitoring*, John Wiley, Hoboken, N. J.

Good, S. A., G. K. Corlett, J. J. Remedios, E. J. Noyes, and D. T. Llewellyn-Jones (2007), The global trend in sea surface temperature from 20 years of Advanced Very High Resolution Radiometer data, *J. Clim.*, *20*(7), 1255–1264, doi:10.1175/JCLI4049.1.

Gottwald, M., et al. (2006), *SCIAMACHY - Monitoring the Changing Earth's Atmosphere*, Inst. fuer Method. der Fernerkundung, Oberpfaffenhofen, Germany.

Grubbs, F. E. (1969), Procedures for detecting outlying observations in samples, *Technometrics*, *11*(1), 1–21, doi:10.2307/1266761.

Guerreiro, C., J. Horálek, F. D. Leeuw, C. Hak, C. Nagl, P. Kurfürst, and J. Ostatnická (2010), Status and trends of NO$_2$ ambient concentrations in Europe, technical report, Eur. Topic Cent. on Air and Clim. Change, Bilthoven, Netherlands.

Heirtzler, J. (2002), The future of the South Atlantic anomaly and implications for radiation damage in space, *J. Atmos. Solar Terr. Phys.*, *64*(16), 1701–1708, doi:10.1016/S1364-6826(02)00120-7.

Kim, S.-W., et al. (2006), Satellite-observed U.S. power plant NO$_x$ emission reductions and their impact on air quality, *Geophys. Res. Lett.*, *33*, L22812, doi:10.1029/2006GL027749.

Kim, S.-W., et al. (2009), NO$_2$ columns in the western United States observed from space and simulated by a regional chemistry model and their implications for NO$_x$ emissions, *J. Geophys. Res.*, *114*, D11301, doi:10.1029/2008JD011343.

Konovalov, I. B., M. Beekmann, J. P. Burrows, and A. Richter (2008), Satellite measurement based estimates of decadal changes in European nitrogen oxides emissions, *Atmos. Chem. Phys.*, *8*, 2623–2641, doi:10.5194/acpd-8-2013-2008.

Konovalov, I. B., M. Beekmann, A. Richter, J. P. Burrows, and A. Hilboll (2010), Multi-annual changes of NO$_x$ emissions in megacity regions: Nonlinear trend analysis of satellite measurement based estimates, *Atmos. Chem. Phys.*, *10*, 8481–8498.

Lamsal, L. N., R. V. Martin, A. van Donkelaar, E. A. Celarier, E. J. Bucsela, K. F. Boersma, R. Dirksen, C. Luo, and Y. Wang (2010), Indirect validation of tropospheric nitrogen dioxide retrieved from the OMI satellite instrument: Insight into the seasonal variation of nitrogen oxides at northern midlatitudes, *J. Geophys. Res.*, *115*, D05302, doi:10.1029/2009JD013351.

Levelt, P., G. van den Oord, M. Dobber, A. Malkki, P. Stammes, J. Lundell, and H. Saari (2006), The Ozone Monitoring Instrument, *IEEE Trans. Geosci. Remote Sens.*, *44*(5), 1093–1101, doi:10.1109/TGRS.2006.872333.

Lin, B.-Q., and J.-H. Liu (2010), Estimating coal production peak and trends of coal imports in China, *Energy Policy*, *38*(1), 512–519, doi:10.1016/j.enpol.2009.09.042.

Lin, J.-T., and M. B. McElroy (2011), Detection from space of a reduction in anthropogenic emissions of nitrogen oxides during the Chinese economic downturn, *Atmos. Chem. Phys.*, *11*(15), 8171–8188, doi:10.5194/acp-11-8171-2011.

Mareckova, K., R. Wankmueller, M. Anderl, S. Poupa, and M. Wieser (2009), Inventory Review 2009 - Emission data reported under the LRTAP Convention and NEC Directive: Stage 1 and 2 review. Status of gridded data and LPS data, technical report, Cent. on Emiss. Invent. and Proj., Vienna.

Mijling, B., R. J. van der A, K. F. Boersma, M. Van Roozendael, I. De Smedt, and H. M. Kelder (2009), Reductions of NO$_2$ detected from space during the 2008 Beijing Olympic Games, *Geophys. Res. Lett.*, *36*, L13801, doi:10.1029/2009GL038943.

Munro, R., M. Eisinger, C. Anderson, J. Callies, E. Corpaccioli, R. Lang, A. Lefebvre, Y. Livschitz, and A. Albiñana Perez (2006), GOME-2 on MetOp, paper presented at 2006 EUMETSAT Meteorological Satellite Conference, EUMETSAT, Helsinki.

Petritoli, A., et al. (2004), First comparison between ground-based and satellite-borne measurements of tropospheric nitrogen dioxide in the Po basin, *J. Geophys. Res.*, *109*, D15307, doi:10.1029/2004JD004547.

Richter, A., and J. P. Burrows (2002), Tropospheric NO₂ from GOME measurements, *Adv. Space Res.*, *29*(11), 1673–1683, doi:10.1016/S0273-1177(02)00100-X.

Richter, A., J. P. Burrows, H. Nüss, C. Granier, and U. Niemeier (2005), Increase in tropospheric nitrogen dioxide over China observed from space, *Nature*, *437*(7055), 129–132, doi:10.1038/nature04092.

Santer, B., T. Wigley, J. Boyle, D. Gaffen, J. Hnilo, D. Nychka, D. Parker, and K. Taylor (2000), Statistical significance of trends and trend differences in layer-average atmospheric temperature time series, *J. Geophys. Res.*, *105*(D6), 7337–7356.

Seinfeld, J. H., and S. N. Pandis (2006), *Atmospheric Chemistry and Physics: From Air Pollution to Climate Change*, 1203 pp., John Wiley, Hoboken, N. J.

Sen, P. K. (1968), Estimates of the regression coefficient based on Kendall's Tau, *J. Am. Stat. Assoc.*, *63*, 1379–1389.

Simpson, D., H. Fagerli, J. Jonson, S. Tsyro, and P. Wind (2003), Transboundary acidification, eutrophication and ground level ozone in Europe - Part I - Unified EMEP model description, *Tech. Rep. 1/2003*, Norw. Meteorol. Inst., Oslo.

Tiao, G., G. C. Reinsel, X. Daming, J. H. Pedrick, Z. Xiaodong, A. J. Miller, J. J. DeLuisi, C. L. Mateer, and D. J. Wuebbles (1990), Effects of autocorrelation and temporal sampling schemes on estimates of trend and spatial correlation, *J. Geophys. Res.*, *95*(D12), 20,507–20,517.

Union des Aéroports Français (2012), Statistiques annuelles, report, Paris. [Available at http://www.aeroport.fr/les-aeroports-de-l-uaf/stats-beauvais-tille.php.]

van der A, R. J., D. H. M. U. Peters, H. Eskes, K. F. Boersma, M. Van Roozendael, I. De Smedt, and H. M. Kelder (2006), Detection of the trend and seasonal variation in tropospheric NO₂ over China, *J. Geophys. Res.*, *111*, D12317, doi:10.1029/2005JD006594.

van der A, R. J., H. J. Eskes, K. F. Boersma, T. P. C. van Noije, M. Van Roozendael, I. De Smedt, D. H. M. U. Peters, and E. W. Meijer (2008), Trends, seasonal variability and dominant NOₓ source derived from a ten year record of NO₂ measured from space, *J. Geophys. Res.*, *113*, D04302, doi:10.1029/2007JD009021.

Vestreng, V., K. Breivik, M. Adams, A. Wagner, J. Goodwin, O. Rozovskaya, and J. M. Pacnya (2005), Inventory Review 2005 - Emission data reported to LRTAP Convention and NEC Directive - Inital review for HMs and POPs, technical report, Norw. Meteorol. Inst., Oslo.

Vestreng, V., L. Ntziachristos, A. Semb, S. Reis, I. S. A. Isaksen, and L. Tarrasón (2009), Evolution of NOₓ emissions in Europe with focus on road transport control measures, *Atmos. Chem. Phys.*, *9*, 1503–1520.

Weatherhead, E., et al. (1998), Factors affecting the detection of trends: Statistical considerations and applications to environmental data, *J. Geophys. Res.*, *103*(D14), 17,149–17,161, doi:10.1029/98JD00995.

Zhang, Q., D. G. Streets, and K. He (2009), Satellite observations of recent power plant construction in Inner Mongolia, China, *Geophys. Res. Lett.*, *36*, L15809, doi:10.1029/2009GL038984.

Zhou, Y., D. Brunner, C. Hueglin, S. Henne, and J. Staehelin (2012), Changes in OMI tropospheric NO₂ columns over Europe from 2004 to 2009 and the influence of meteorological variability, *Atmos. Environ.*, *46*(2), 482–495, doi:10.1016/j.atmosenv.2011.09.024.